

# The Effects of Fused Deposition Modeling Process Parameters on the Complex Modulus of 3D Printed ABS

R. Vahed<sup>1</sup>, H.R. Zareie Rajani<sup>1,2</sup>, A.S. Milani<sup>1\*</sup>

<sup>1</sup> Composites Research Network-Okanagan Laboratory, School of Engineering,  
University of British Columbia, Kelowna, Canada

<sup>2</sup> Global Heat Transfer Ltd., R&D Department, Edmonton, Canada

\*Corresponding author ([abbas.milani@ubc.ca](mailto:abbas.milani@ubc.ca))

**Keywords:** *Additive Manufacturing (AM), Fused Deposition Modeling (FDM), Acrylonitrile Butadiene Styrene (ABS), Complex Modulus*

## ABSTRACT

Additive manufacturing (AM) has become a mainstream composite manufacturing process due to its ability to build 3-Dimensional parts with complex geometries from thermoplastics, without producing minimal waste. In order to predict and consequently control the mechanical behavior of parts fabricated by Fused Deposition Modeling (FDM), as one of the most common AM methods, it is necessary to understand the effects of process parameters on the final properties of forming consumables. This article presents an experimental approach to investigate the effects of four FDM parameters (including temperature, raster orientation, layer height, and deposition speed as control variables) on the complex modulus of processed Acrylonitrile Butadiene Styrene (ABS) filaments. A Taguchi design of experiment (DOE) approach is employed along with the Dynamic Mechanical analysis (DMA). Results through a Lenth's method, used for the statistical analysis of unreplicated (costly) experiments, showed that during FDM as the material approaches its glass transition temperature, the feeding rate becomes a more significant factor affecting the complex modulus, followed closely by the raster orientation, and then the nozzle temperature and the layer height. Additionally, it was found that mechanical performance of the final part can drop as high as 50%-80% under different FDM conditions, when compared to the un-processed filaments. This suggests that the integration of manufacturing and design aspects should be considered more critically when using the AM technology, in comparison to conventional thermoplastic manufacturing techniques.

## 1 INTRODUCTION

Additive Manufacturing (AM) has been viewed as a novel manufacturing method, as opposed to subtractive manufacturing techniques, to produce three dimensional objects with minimal material waste [1]. In this process, Computer Aided Design (CAD) files that contain 3D part models are employed as data input. The 3D CAD model is first sliced into several 2D layers and then submitted to a 3D printer, which then fabricates each 2D layer and joins them one upon another, to make the final part. The Fused Deposition Modelling (FDM) is one of the most common AM techniques used in industry [2]. In this technology (Figure 1), a nozzle, placed in print head, melts/highly softens the thin thermoplastic filaments and deposits them on a horizontal plane (bed) to form a 2D layer. Once each layer is printed and consolidated, a relative motion along Z axis allows the printer to form the next layer and build the entire 3D model [3]. Although the FDM is mainly used for rapid prototyping, a series of attempts has been lately seen to enable manufacture of end use parts at mass scale [4]. Numerous studies have focused on selection of the optimized

set of process parameters through understanding the role of the FDM on the mechanical properties of 3D printed objects [5-9]. Some of the most frequently reported FDM process parameters include (see also Figure1):

- 1) road width ( $w$ ); that is the width of a road deposited through the nozzle,
- 2) layer thickness ( $t$ ); that is the thickness of each 2D layer during printing,
- 3) feeding rate ( $v$ ); that is the rate at which the thermoplastic filament is fed into the nozzle,
- 4) forming temperature ( $T$ ); that is the temperature of the material and nozzle's exit,
- 5) raster orientation ( $\theta$ ); that is the orientation of roads in each 2D layer,
- 6) overlap ( $b$ ); that is the amount of overlap between two adjacent roads, and
- 7) nozzle diameter ( $d$ ).

Despite the fact that most thermoplastics are viscoelastic, dynamic mechanical properties of 3D printed parts have not attracted attentions amongst researchers as extensive as their static mechanical properties. Arivazhagan et al.[7] used a Dynamic Mechanical Analyzer (DMA) to examine the effect of road width, raster orientation, and temperature on the viscosity and dynamic moduli of the FDM processed ABS samples. In another study, Mohamed et al.[10] considered layer thickness, overlap, raster angle, raster orientation, and road width as control factors to investigate the dynamic mechanical properties of the FDM processed ABS. The effect of some other important parameters such as feeding rate has not been addressed. In addition, a lack of systematic experimental design often does not allow for parametric studies to account for a *statistically-informed* selection of factor combinations. This can potentially lead to errors in interpreting the role of each process parameters. This article presents a designed experimental approach to investigate the concurrent effects of four FDM process parameters including temperature, raster orientation, layer thickness, and feeding rate, on the dynamic mechanical properties of the FDM processed ABS. Specifically, a combination of Dynamic Mechanical Analyzer (DMA) and a Taguchi DOE with Lenth's method has been employed to reveal the level of significance of FDM parameters on altering the complex modulus of ABS filaments. Not only does the DOE minimize the number of required tests for process optimization, but also it provides a visual inspection of the parameter sets that can maximize the response (here the complex modulus).

## 2 METHODOLOGY

### 2.1 Theoretical background

Generally, elastic materials like most metals show their response in accordance to the applied stress, whereas the response of viscoelastic materials like polymers is affected by both the current and past states (history) of stress [11]. The macro-level viscoelastic material models often employ spring and dashpots as equivalent elasticity and viscosity elements, allowing to model both steady state and transient response of the material to an applied stress. One major tool to investigate the viscoelasticity of materials is the Dynamic Mechanical Analyzer (DMA). During DMA testing, the material sample is subjected to e.g. a sinusoidal strain,  $\varepsilon$ , with a frequency of  $\omega$ . If the material is purely elastic, its stress response,  $\sigma$ , would be directly proportional to the applied strain with no lag [12]. However, viscoelastic materials show a delayed response to the oscillatory strain (Figure 2) which can be formulated as [13]:

$$\varepsilon = \varepsilon_0 \sin(\omega t) \quad (1)$$

$$\sigma = \sigma_0 \sin(\omega t + \delta) \quad (2)$$

Where  $t$  represents time,  $\varepsilon_0$  and  $\sigma_0$  are the magnitudes of strain and stress functions, respectively. The phase angle,  $\delta$ , represents the damping ability of the material. By defining the ratio of maximum stress to the maximum strain as the complex modulus ( $E^*$ ), the stress response can be re-written as:

$$\sigma = \varepsilon_0 E^* \sin(\omega t + \delta) \quad (3)$$

The complex modulus, as a viscoelastic material property, consists of two components: the real part and the imaginary part. The real part is known as the storage modulus ( $E'$ ) which characterizes the elastic behavior of the material. The imaginary part is known as the loss modulus ( $E''$ ) which is utilized to interpret the viscos behavior of the material. The relationship between these moduli is given as (also see Figure3):

$$E^* = E' + iE'' \quad (4)$$

### 2.2 Experimental procedure

The FDM fabrications were carried out based on an L-16 orthogonal DOE array [14] and under the combination of the four process parameters: raster orientation, layer height, feeding rate, and the nozzle temperature. The visual inspection of samples and also the needs defined by the industrial partner led to selection of these specific control factors. The allowable minimum and maximum set up suggested by the 3-D printer manufacturer (Maker gear M2 3D) led to the choice of factor levels shown in Table 1. Table 2 outlines the ensuing full experimental layout. The filaments were made of ABS supplied by Stratasys Ltd, with a nominal diameter of 1.75 mm. In order to perform the dynamic mechanical analyses, rectangular samples with the size of  $57 \times 14 \times 1.25\text{mm}^3$  (length  $\times$  width  $\times$  thickness) were modeled by SolidWorks and printed. Amorphous plastics such as ABS are easy to thermoform, they soften over a range of forming temperatures (they have no melting point), and tend to have good dimensional stability. To characterize the FDM processed ABS material, the mechanical analyses were carried out by a DMA Q800, at the dual cantilever bending mode. For comparison purposes, the DMA tests were also conducted on unprocessed ABS filaments (i.e. as the control group) with the length of 57mm. All tests were performed at standard room condition per ISO R291.

## 3 RESULTS AND DISCUSSION

The observed trends of complex modulus versus temperature for all the FDM processed and unprocessed ABS samples are depicted in Figure 4. According to the distinct trends seen between processed and unprocessed samples, it can be concluded that the FDM reduces the magnitude of complex modulus regardless of the combination of process parameters used. This change is specifically clear at lower temperatures. For instance, according to Figure 5 the complex modulus has dropped from 2732.11 MPa at 40°C to 1046.14 MPa under ABS 9 (i.e., a 62% reduction). This reduction at the glass transition temperature,  $T_g$ , according to Figure 6, has reached to about 80%. Although the FDM process seems to unavoidably decrease the complex modulus, by selecting a suitable set of process parameters, this reduction can be minimized. The numerical values of complex modulus at the two selected working temperatures (40°C and  $T_g$ ) are also listed in Table 3, which will be employed in the Lenth's method in the following section.  $T_g$  serves as an important material property representing a transition point between the glassy and rubbery behaviors for amorphous or semi-crystalline polymers [7] (note that for purely crystalline polymers no  $T_g$  occurs). While increasing the temperature to transit from glassy region to the rubbery region, the damping ability of the material (often measured via  $\tan \delta$ ) reaches to its local peak and then drops suddenly. For the ABS filaments, the  $T_g$  was obtained for each test, with the average being around 108°C. This limiting temperature, is considered as the maximum working temperature during service of a part after it is printed. Conversely, during thermoforming, as the material cools down from the melt state to the rubbery state, most deformations are desired to take place before reaching the  $T_g$ .

Figures 7 and 8 provide detailed view of the effect of each process parameter on the complex modulus of the FDM processed parts. Based on Figure 7, the raster orientation is the most influential factor to change the complex modulus at working temperature of 40°C. The zero-degree raster orientation has given the highest complex modulus, while increasing the raster orientation up to 45° drops the modulus. Using a bi-directional raster orientation ( $\pm 45^\circ$ ) could not improve the modulus. A higher value of the complex modulus was obtained when the layer height was at 130

microns. The maximum complex modulus for the FDM processed part was achieved when the nuzzle temperature was set at 270°C. By increasing the nuzzle temperature above this point, the complex modulus decreased, and again increased. Increasing the feeding rate enhanced the complex modulus up to the feed rate of 3000 mm/min, after which it decreased. Similar factor effect analyses could be attained for the case of working temperature at  $T_g$ , according to Figure 8. Comparison of Figures 7 and 8 clearly shows that there is no unique set of parameters that can globally maximize the modulus at both working temperatures.

Next, in order to statistically assess the significance level of process parameters, the Lenth's method was employed, as a powerful tool to analyze experiments with single replicate factorial design [15]. Assume in a factorial design,  $m$  effects exist for both main factors and interactions. These effects are referred to as  $c_1, c_2, \dots, c_m$ . For a  $2^k$  full factorial design,  $m = 2^k - 1$ . Lenth's method defines a numerical value called the Pseudo Standard Error (PSE) as.

$$PSE = 1.5 \text{ median}(|c_j|: |c_j| < 2.5S_0) \quad (5)$$

Where,

$$S_0 = 1.5 \text{ median}(|c_j|) \quad (6)$$

In essence, PSE is a measure estimating the variation of effects. The margin of error (ME) is defined by:

$$ME = t_{\frac{\alpha}{2}, d} PS \quad (7)$$

Where  $t_{\frac{\alpha}{2}, d}$  is the t-distribution with the significance level of  $\alpha$  and the degree of freedom of  $d = \frac{m}{3}$ . Finally, for a specific factor, if the absolute value of the effect is greater than  $ME$ , that factor is considered significant in changing the response.

The Lenth's approach was employed to find the significant FDM parameters on  $E^*$  at  $T_g$  and at 40°C, and to rank them with respect to their significance levels (Tables 4 and 5). The value provided in each cell of this table represents the mean value of complex modulus with respect to different levels of each parameter. The delta parameter that in each column indicates the difference between the corresponding maximum and minimum values, which is considered as the given factor's effect. From Tables 4 and 5 it can be concluded that all the four process parameters have significant effects on the mechanical properties of 3D printed parts. The raster orientation is ranked first, followed by the layer height, feeding rate, and nozzle temperature, for the case of 40°C working temperature. However, at a working temperature coincident with  $T_g$ , this order of factors changes such that the feeding rate becomes the most significant factor, followed closely by the raster orientation. The temperature of the nozzle and the layer height are ranked third and fourth, respectively. This again clearly shows that for a global prediction and optimization of the FDM process, especially when the number and level of parameters increase, more sophisticated learning tools (e.g., neural networks) should be adapted in future studies.

## 4 CONCLUSIONS

This work undertook an investigation into the influence of FDM process parameters on the complex modulus of 3D printed parts. Raster orientation, temperature, layer height and feeding rate were selected as four important control factors. A Taguchi DOE approach was employed to reduce the number of tests as making one sample for each printing setup is time and cost consuming. For each process parameter, four levels were assigned and accordingly 16 different samples (via an L-16 orthogonal array) were built to test their complex modulus, using the DMA. According to the results, the FDM process changes the magnitude of complex modulus drastically, while keeping the general trend of modulus-temperature curves (e.g., the  $T_g$  did not change noticeably before and after applying the process). The effect

of process parameters on the modulus at two selected working temperatures were investigated. Based on the Lenth's method, it was found that the feeding rate and raster orientation are comparably the most significant factors to control  $E^*$  at glass transition temperature, followed by the nozzle temperature and the layer height. On the other hand, the complex modulus variation at other temperatures (e.g., 40°C) was found to be distinctly controlled by the raster orientation as the first ranked factor. This means that, as the state of the material changes from glassy to the rubbery, the feeding rate becomes more effective to control the mechanical properties of the 3D printed part. Interestingly, it was found that the material response to all the four process parameters is non-linear, and at each working temperature, the optimum point mostly lies within the mid-levels of factors. It is believed that the use of advanced machine learning techniques can be highly useful for optimization of such complex manufacturing processes as FDM.

### 5 REFERENCES

- [1] Standard- F2792 12a, 2012, "Standard Terminology for Additive Manufacturing Technologies," *ASTM International, West Conshohocken, PA, Doi*, vol. 10.
- [2] Z. Doubrovski, J. C. Verlinden and J. M. Geraedts, "Optimal design for additive manufacturing: Opportunities and challenges," in *ASME 2011 International Design Engineering Technical Conferences and Computers and Information in Engineering Conference*, pp. 635-646, 2011.
- [3] I. Gibson, D. W. Rosen and B. Stucker, "*Additive Manufacturing Technologies*". Springer, 2010.
- [4] I. Campbell, D. Bourell and I. Gibson, "Additive manufacturing: rapid prototyping comes of age," *Rapid Prototyping Journal*, vol. 18, pp. 255-258, 2012.
- [5] A. Bagsik, V. Schöppner and E. Klemp, "FDM part quality manufactured with ultem\* 9085". in *14th International Scientific Conference on Polymeric Materials*, 2010.
- [6] M. K. Agarwala *et al*, "Structural quality of parts processed by fused deposition". *Rapid Prototyping Journal*, vol. 2, pp. 4-19, 1996.
- [7] A. Arivazhagan and S. Masood, "Dynamic mechanical properties of ABS material processed by fused deposition modelling". *Int J Eng Res Appl*, vol. 2, pp. 2009-2014, 2012.
- [8] S. Ahn *et al*, "Anisotropic material properties of fused deposition modeling ABS". *Rapid Prototyping Journal*, vol. 8, pp. 248-257, 2002.
- [9] B. Lee, J. Abdullah and Z. Khan, "Optimization of rapid prototyping parameters for production of flexible ABS object". *J. Mater. Process. Technol.*, vol. 169, pp. 54-61, 2005.
- [10] O. A. Mohamed *et al*, "Effect of Process Parameters on Dynamic Mechanical Performance of FDM PC/ABS Printed Parts Through Design of Experiment". *Journal of Materials Engineering and Performance*, pp. 1-14.
- [11] J. D. Ferry, "*Viscoelastic Properties of Polymers*". John Wiley & Sons, 1980.
- [12] K. P. Menard, "*Dynamic Mechanical Analysis: A Practical Introduction*." CRC press, 2008.
- [13] M. Meunier and R. Sheno, "Dynamic analysis of composite sandwich plates with damping modelled using high-order shear deformation theory". *Composite Structures*, vol. 54, pp. 243-254, 2001.
- [14] G. Taguchi, S. Chowdhury and Y. Wu, "Quality Engineering: The Taguchi Method". *Taguchi's Quality Engineering Handbook*, pp. 56-123, 2007.
- [15] D. C. Montgomery, "*Design and Analysis of Experiments*". John Wiley & Sons, 2008.

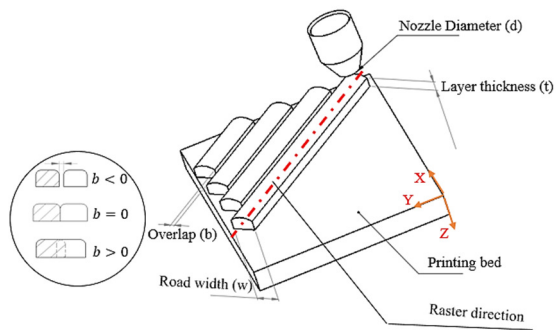


Figure 1. Schematic view of the FDM process and its parameters

Control factors	Levels			
	Level 1	Level 2	Level 3	Level 4
Raster orientation	0°	90°	45°	±45°
Layer height (μm)	50	130	210	300
Temperature (°C)	250	270	290	310
Feeding rate (mm/min)	1000	2000	3000	4000

Table 1. Process parameters and their corresponding levels

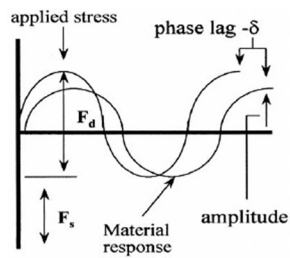


Figure 2. The graphical relationship between stress and strain in viscoelastic material [12]

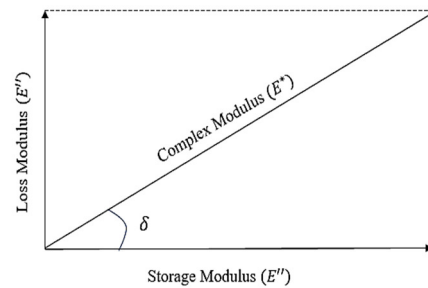


Figure 3. The vector projection of dynamic moduli [13]

Experiment	Raster orientation	Layer height (μm)	Nozzle Temperature (°C)	Feed rate (mm/min)	Experiment	Raster orientation	Layer height (μm)	Nozzle Temperature (°C)	Feed rate (mm/min)
<b>1</b>	1	1	1	1	<b>9</b>	3	1	3	4
<b>2</b>	1	2	2	2	<b>10</b>	3	2	4	3
<b>3</b>	1	3	3	3	<b>11</b>	3	3	1	2
<b>4</b>	1	4	4	4	<b>12</b>	3	4	2	1
<b>5</b>	2	1	2	3	<b>13</b>	4	1	4	2
<b>6</b>	2	2	1	4	<b>14</b>	4	2	3	1
<b>7</b>	2	3	4	1	<b>15</b>	4	3	2	4
<b>8</b>	2	4	3	2	<b>16</b>	4	4	1	3

Table 2. Experimental layout based on the Taguchi L-16 design

## The Effects of Fused Deposition Modeling Process Parameters on the Complex Modulus of 3D Printed ABS

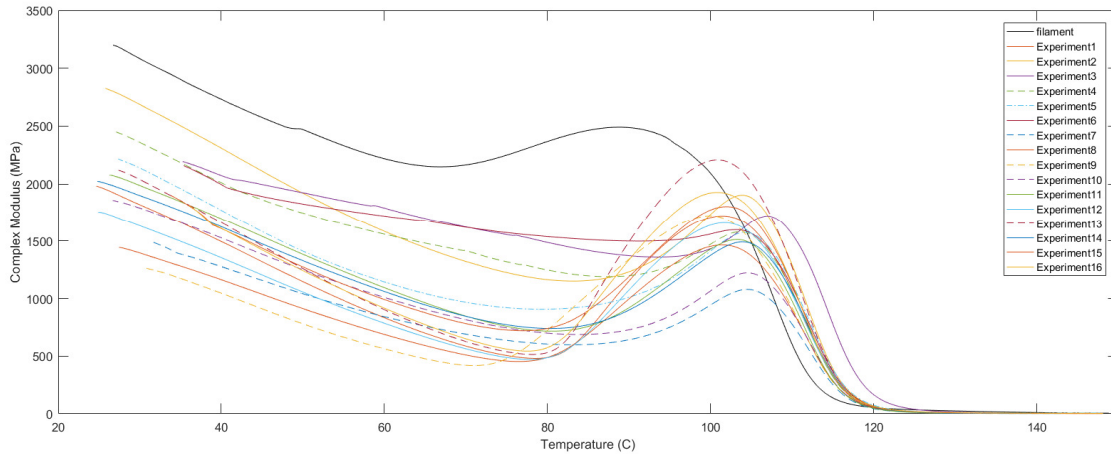


Figure 4. The variation of measured complex modulus as a function of temperature for the FDM processed and unprocessed ABS

Test	Complex modulus at $T_g$	Complex modulus at 40°C	Test	Complex modulus at $T_g$	Complex modulus at 40°C
1	66.22	1495.78	9	62.81	1046.148
2	82.77	2309.60	10	57.11	1526.87
3	136.69	2068.87	11	64.60	1695.74
4	72.93	2010.91	12	86.93	1354.30
5	83.74	1771.19	13	94.42	1663.74
6	85.73	1994.91	14	65.95	1624.91
7	48.60	1276.78	15	120.26	1606.74
8	83.00	1162.86	16	103.95	1610.27
			<b>Unprocessed ABS</b>	259.33	2732.11

Table 3. Complex modulus at working temperatures of 40°C and at  $T_g$  for the FDM processed and unprocessed ABS

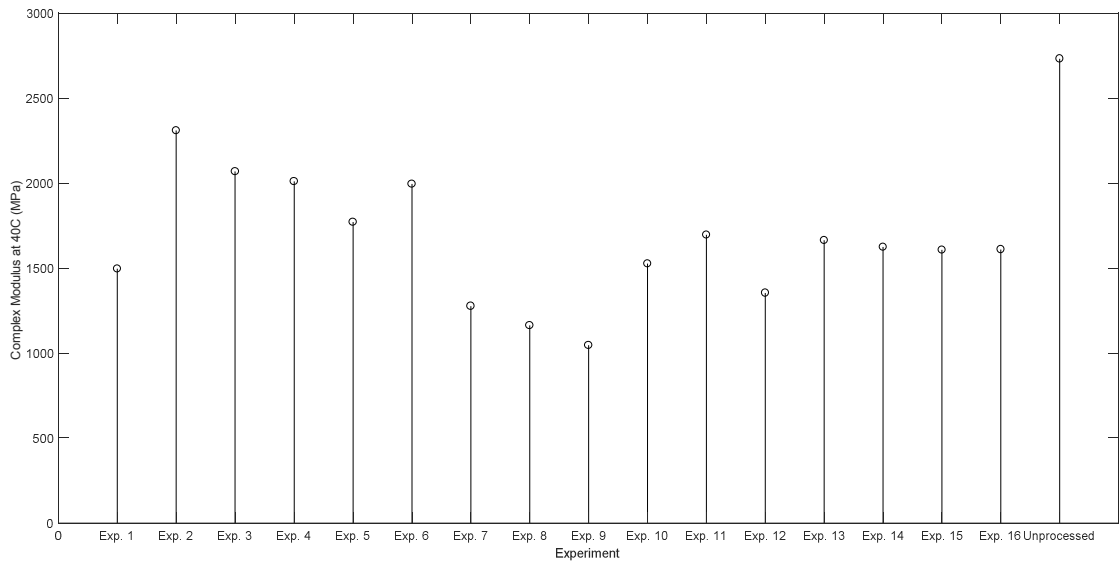


Figure 5. The variation of complex modulus at working temperature of 40°C for the FDM processed and unprocessed ABS

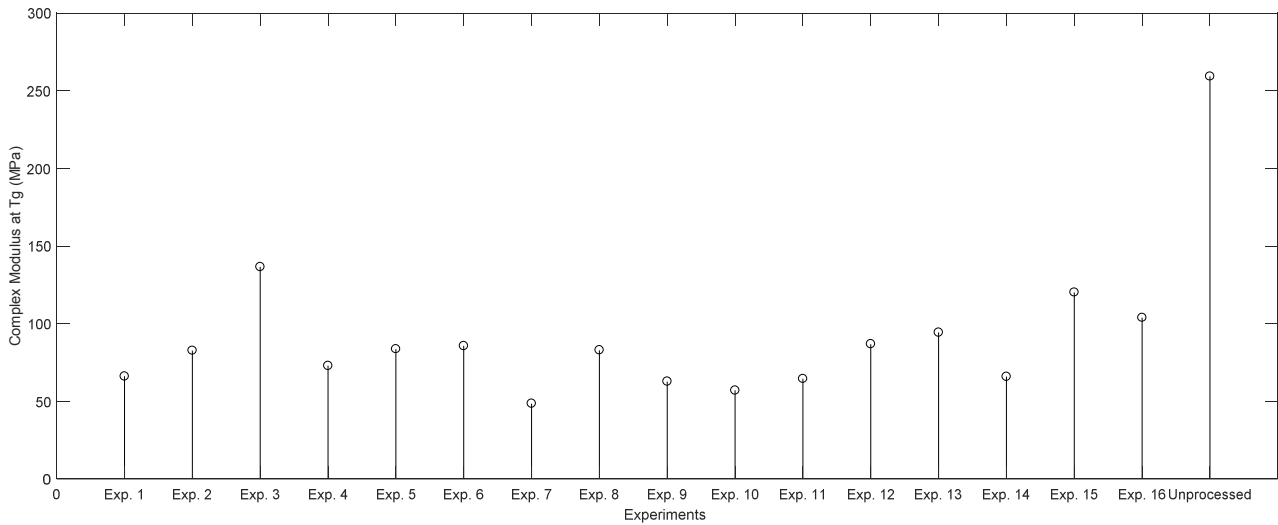


Figure 6. The variation of complex modulus at working temperature of  $T_g$  for the FDM processed and unprocessed ABS

## The Effects of Fused Deposition Modeling Process Parameters on the Complex Modulus of 3D Printed ABS

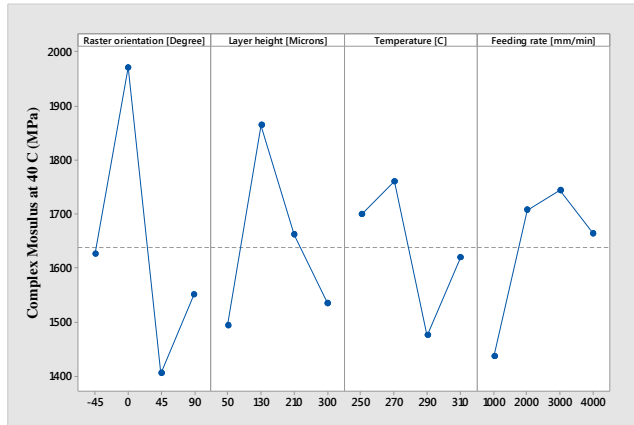


Figure 7. The effect of each process parameter on the complex modulus at working temperature of 40°C

Level	Raster orientation	Layer height	Nuzzle temperature	Feed rate
1	1971	1494	1699	1438
2	1551	1864	1760	1708
3	1406	1662	1476	1744
4	1626	1535	1620	1665
Range	566	370	285	306
Rank	1	2	4	3
ME threshold	248	248	248	248

Table 4. Lenth's method of factor analysis for complex modulus response at working temperature of 40°C; the values for factor levels correspond to the average of response under each corresponding level according to Tables 2 and 3; the physical values of factor levels are given in Table 1.

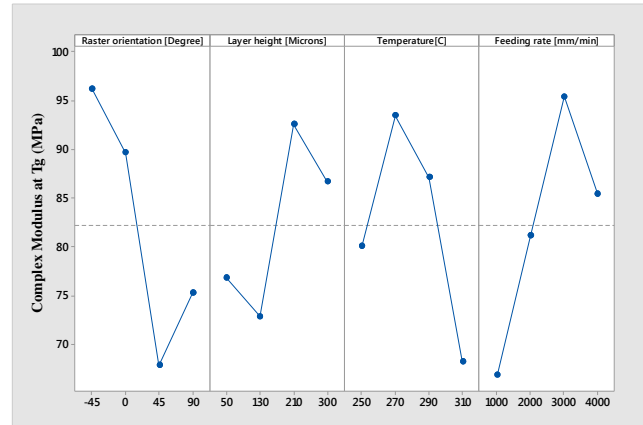


Figure 8. The effect of each process parameter on the complex modulus at working temperature of  $T_g$

Level	Raster orientation	Layer height	Nuzzle temperature	Feed rate
1	89.66	76.8	80.13	66.93
2	75.27	72.9	93.43	81.2
3	67.87	92.54	87.12	95.38
4	96.15	86.71	68.27	85.44
Range	28.28	19.64	25.16	28.45
Rank	2	4	3	1
ME Threshold	19	19	19	19

Table 5. Lenth's method of factor analysis for complex modulus response at working temperature of  $T_g$ ; the values for factor levels correspond to the average of response under each corresponding level according to Tables 2 and 3; the actual physical values of factor levels are given in Table 1.